Nanoscopy of Filamentous Actin in Cortical Dendrites of a Living Mouse

Katrin I. Willig,[†‡*] Heinz Steffens,[†] Carola Gregor,[†] Alexander Herholt,[¶] Moritz J. Rossner,[¶] and Stefan W. Hell[†‡*]
[†]Department of NanoBiophotonics, Max Planck Institute for Biophysical Chemistry, Göttingen, Germany; [‡]Center for Nanoscale Microscopy and Molecular Physiology of the Brain, Göttingen, Germany; and [¶]Department of Molecular Neurobiology and Department of Psychiatry, Ludwig-Maximilians-University, München, Germany

ABSTRACT We demonstrate superresolution fluorescence microscopy (nanoscopy) of protein distributions in a mammalian brain in vivo. Stimulated emission depletion microscopy reveals the morphology of the filamentous actin in dendritic spines down to 40 μm in the molecular layer of the visual cortex of an anesthetized mouse. Consecutive recordings at 43–70 nm resolution reveal dynamical changes in spine morphology.

Received for publication 19 August 2013 and in final form 13 November 2013.

*Correspondence: kwillig@gwdg.de or shell@gwdg.de

The postsynaptic part of most excitatory synapses in the brain is formed by dendritic spines, which are small protrusions along the dendrites that are highly dynamic during development, but also undergo morphological changes in adulthood (1,2). A prime candidate for regulating these dynamics is the neuronal actin network (3). Filamentous (F-) actin is also important for anchoring postsynaptic receptors and modulating synaptic activities, e.g., through the organization of the postsynaptic density (3). Clearly, the actin dynamics of dendritic spines is best studied in vivo, e.g., in a living mouse, and with confocal and multiphoton microscopy because these techniques can provide three-dimensional optical sectioning several 100 μm inside brain tissue (4). However, because necks of dendritic spines are on the 50–150-nm scale, their details are beyond the 250–400-nm resolution afforded by these diffraction-limited techniques. Fortunately, the diffraction resolution barrier of lens-based fluorescence microscopy has recently been overcome by causing the fluorophores of nearby features to emit sequentially (5). One of the techniques relying on this principle, stimulated emission depletion (STED) microscopy, has recently resolved dendritic spines in the cortex of a living mouse (6). In that initial, in vivo superresolution study, the dendrites were only volume-labeled, and consequently, the spatial arrangements of specific cytoskeletal proteins could not be imaged. On the other hand, F-actin has actually been imaged in living brain slices (7), but in vivo imaging of these structures has not yet been attained.

Compared to other superresolution or nanoscopy techniques, STED microscopy bears a number of advantages for imaging spines in the living brain. Implemented as a beam scanning confocal microscope, STED nanoscopy offers optical sectioning and measurements at greater depth. In addition, motion artifacts of the dynamic structures can be minimized by fast scanning. And last but not least, STED can be performed with standard fluorescent proteins. Therefore, we here apply STED nanoscopy to noninvasively uncover the actin cytoskeleton in the living mouse brain. In particular, we show that the 43–70-nm resolution obtained by STED visualizes rearrangements of the dendritic spines in vivo.

We took on the challenge of labeling the actin cytoskeleton in the living mouse cortex. We utilized Lifeact-EYFP, a fusion protein consisting of a small peptide and the yellow fluorescent protein EYFP, which directly binds to F-actin without disturbing its polymerization (8). The labeling itself was accomplished by viral infection. To this end, adeno-associated viral particles (AAV) of serotype 2, facilitated by the neuron specific human *synapsin* promoter hSYN (9) and Semliki Forest viruses (SFV), were created to express Lifeact-EYFP in neurons. For virus injection, the mouse was anesthetized and the head was fixed in a model No. SG-4N head holder (Narishige International USA, East Meadow, NY). A 5-mm incision of the skin of the head enabled drilling a 0.5-mm-diameter hole into the skull. The hole was positioned 0.5 mm outside the prospective imaging center in the visual cortex. The AAVs were injected with a micropipette connected to a pressure generator (Tooheyspritzer; Toohey Company, Fairfield, NJ). Thus, we were able to inject ~750 nL of concentrated AAV at an angle of 30° over a time of ~5 min to the layer of pyramidal cells in the prospective imaging center. After injection and 5-min pause, the pipette was retracted with a 5-min break at the half-way point to allow the virus to diffuse into the tissue. The skin was closed with three stitches and the mouse kept on a heating plate in an anesthetic recovery box until wake-up.

Editor: David Piston.

http://dx.doi.org/10.1016/j.bpj.2013.11.1119

After 10 days the mouse was prepared for in vivo STED nanoscopy, according to Berning et al. (6) (see also the Supporting Material). At this point, the skin had completely healed and the mouse showed no sign of obvious behavioral abnormality. Optical access was provided by a glass-sealed hole of ~2 mm in diameter, exposing the visual cortex (Fig. 1 *a*). STED nanoscopy was performed with an upright beam-scanning microscope similar to that described by Berning et al. (6), with short optical paths and good vibration-damping (Fig. 1 *b* and see the Supporting Material). The coaligned excitation and STED beams were focused onto the mouse brain using a 1.3 numerical-aperture glycerol immersion lens. The correction collar of the lens allowed compensation of spherical aberrations arising from focusing beneath the brain surface (7).

Fig. 1 *c* shows representative parts of dendrites in the molecular layer of the visual cortex. The combination of Lifeact-EYFP labeling and superresolution displayed the dendritic actin of the living mouse neuron in unprecedented detail. Most spines have an actin-rich bulbous end, i.e., a spine head. Sometimes, the dendrite shows small areas with high actin enrichment, which presumably constitute the beginning of filopodia outgrowths (see Fig. S1 in the Supporting Material). The STED image quality was maintained down to a depth of 40 μm below the cover glass. The actin filaments in the spine neck were 43–70-nm thin (see Fig. S2), which can also be interpreted as an upper estimate (poorest value) for the resolution obtained by STED. Note that the images were not processed after recording. All dendrites appeared normal, i.e., in comparison with the morphology of volume-labeled pyramidal cells of transgenic mice (6). The STED beam average laser power was 34 mW. For somewhat greater laser power, we occasionally saw swelling of the dendrites but they were never destroyed. The maximum applicable power depends on the thickness of the dendrite and most likely on the presence of mitochondria as well.

Next, we raised the expression level of Lifeact-EYFP by replacing AAV with SFV infection (7,10). We injected 750 nL of SFV (see the Supporting Material) analog to the AAV protocol and allowed the mouse to wake up and recover. After one day, we recorded in vivo STED nanoscopy images of the visual cortex. The labeling was sparser than with the AAV, i.e., fewer cells expressed Lifeact-EYFP, but the signal was brighter and highly specific to neurons. Fig. 2 shows a STED image of a part of a dendrite in the visual cortex at depth <10 μm. The actin label is brighter in the spine heads than in the body of the dendrite, showing that Lifeact-EYFP is primarily attached to F-actin. STED recording over 12 min revealed morphological changes in the actin cytoskeleton. No changes were observed after fixation (see Fig. S4). Bleaching-corrected brightness changes in the spine head inherently reflect density changes in the actin network. In contrast to AAV, SFV shuts down host cell protein synthesis, which leads to cell death after >24 h (11,12); this was not improved by the less cytotoxic SFV(PD) variant (11). Therefore, we recorded

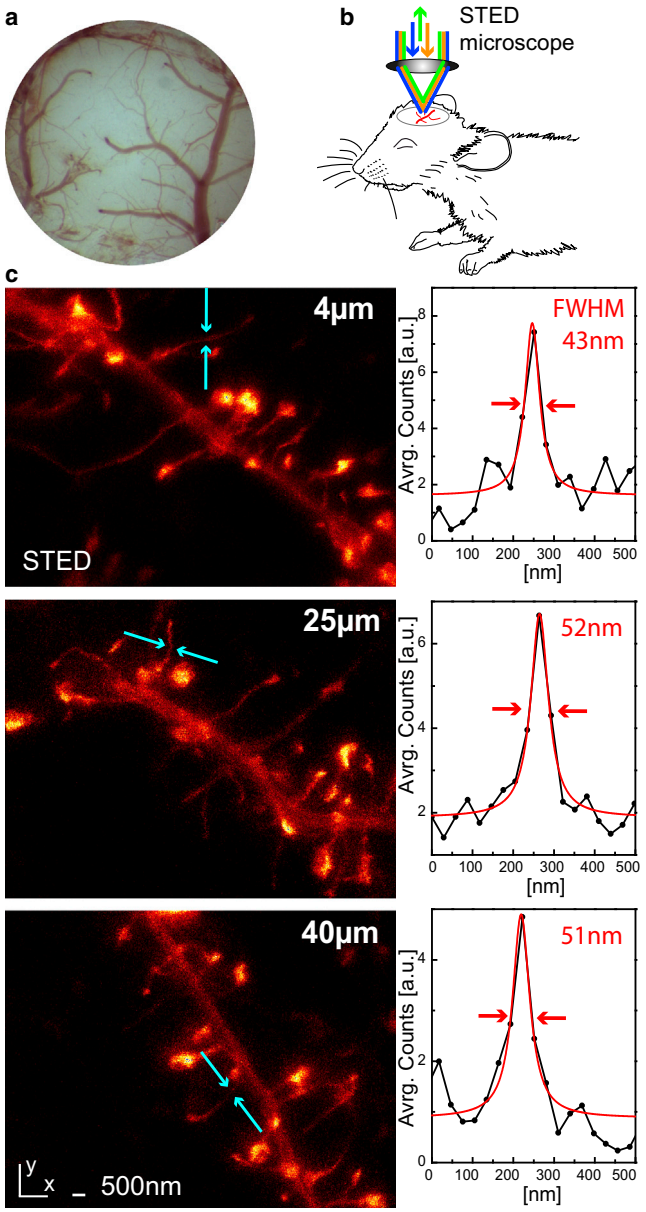

FIGURE 1 STED nanoscopy of the dendritic filamentous (F-) actin cytoskeleton in the visual cortex of a living mouse. (*a*) Clear view of the visual cortex through an optical window. (*b*) Upright STED imaging of the anesthetized mouse. (*c*) Dendritic F-actin in the molecular layer of the visual cortex at 4, 25, and 40-μm depths. Maximum intensity projection of a stack of five (*xy*) images taken in 500-nm axial (*z*) distances. (*Right*) Line profile at the marked positions; average of five lines of the raw data and Lorentz fit with full width at half-maximum (FWHM); all image data are raw.

in vivo nanoscopy images one day after viral transduction where most dendrites looked healthy. To confirm the viral transduction and verify the subtype of the infected neurons, we perfused the mouse with paraformaldehyde and imaged the brain slices of the region of interest (see Fig. S5). Whereas the AAV labeled mainly neurons of the pyramidal layer, the SFV infected sparsely neurons from all layers of the cortex.

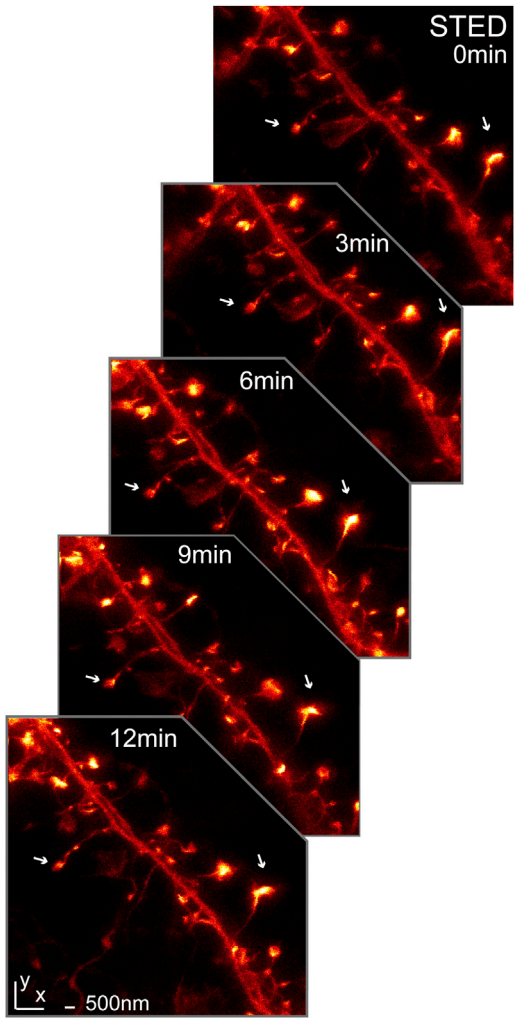

FIGURE 2 Actin rearrangement in dendritic spines at 60-nm subdiffraction spatial resolution. Image stacks reveal dynamic changes of actin in the spines. (*Arrows*) Shape changes of spine heads. Maximum intensity projection of five slices of 500-nm axial (*z*) separation; all data are raw. Average power at back-aperture of objective lens: 2.4 μW excitation and 38-mW STED.

The 4–5-fold lateral resolution improvement of STED over standard confocal and multiphoton microscopy is not sufficient to resolve single actin fibers, as with platinum replica electron microscopy (13). Future refinements of both labeling and STED imaging should make this goal achievable. The resolution along the optical (z) axis was kept diffraction-limited (~500 nm) so that the total illumination dose remained small. At depth >40 μm, scattering and aberrations compromise the image quality. Nonetheless, the molecular layer of the sensory cortex is a highly interesting target for functional optical nanoscopy, because it is the site of the first stage of cortical sensory processing.

In summary, STED microscopy can be applied to study subcellular protein structures at 43–70-nm resolution down to 40 μm in the brain of a living mammal. Specifically, we showed that the dynamic actin network responsible for the morphologic plasticity in the brain can be superresolved in the living mouse. Extending in vivo STED microscopy to other protein assemblies as well as to other cell types should provide basic insights into the working principles of the brain.

SUPPORTING MATERIAL

STED Nanoscopy in the Visual Cortex at Various Depths, Adeno-Associated Virus (AAV), Semliki Forest Virus (SFV), Surgical Preparation, STED Microscopy, Image Artifacts Caused by Vital Functions, Control: STED Microscopy Images After Fixation, Distribution of Infected Neurons after Viral Transduction, and five figures are available at http://www.biophysj.org/biophysj/supplemental/S0006-3495(13)02376-X.

ACKNOWLEDGEMENTS

We thank K. Deisseroth for the pAAV-hSyn-EYFP construct, T. Gilat and A. Rupp for virus production, and E. d'Este for cultured neurons. The experiments were performed according to the guidelines of the national law regarding animal protection procedures and by the responsible authorities, the Niedersächsisches Landesamt für Verbraucherschutz.

Part of the work was supported by the Deutsche Forschungsgemeinschaft Center for Nanoscale Microscopy and Molecular Physiology of the Brain through a grant to S.W.H.

REFERENCES

1. Yuste, R., and T. Bonhoeffer. 2001. Morphological changes in dendritic spines associated with long-term synaptic plasticity. *Annu. Rev. Neurosci.* 24:1071–1089.
2. Bhatt, D. H., S. Zhang, and W.-B. Gan. 2009. Dendritic spine dynamics. *Annu. Rev. Physiol.* 71:261–282.
3. Hotulainen, P., and C. C. Hoogenraad. 2010. Actin in dendritic spines: connecting dynamics to function. *J. Cell Biol.* 189:619–629.
4. Svoboda, K., and R. Yasuda. 2006. Principles of two-photon excitation microscopy and its applications to neuroscience. *Neuron.* 50:823–839.
5. Hell, S. W. 2009. Microscopy and its focal switch. *Nat. Methods.* 6:24–32.
6. Berning, S., K. I. Willig, …, S. W. Hell. 2012. Nanoscopy in a living mouse brain. *Science.* 335:551.
7. Urban, N. T., K. I. Willig, …, U. V. Nägerl. 2011. STED nanoscopy of actin dynamics in synapses deep inside living brain slices. *Biophys. J.* 101:1277–1284.
8. Riedl, J., A. H. Crevenna, …, R. Wedlich-Soldner. 2008. Lifeact: a versatile marker to visualize F-actin. *Nat. Methods.* 5:605–607.
9. Shevtsova, Z., J. M. I. Malik, …, S. Kügler. 2005. Promoters and serotypes: targeting of adeno-associated virus vectors for gene transfer in the rat central nervous system in vitro and in vivo. *Exp. Physiol.* 90:53–59.
10. DiCiommo, D. P., and R. Bremner. 1998. Rapid, high level protein production using DNA-based Semliki Forest virus vectors. *J. Biol. Chem.* 273:18060–18066.
11. Lundstrom, K., C. Schweitzer, …, M. U. Ehrengruber. 2001. Semliki Forest virus vectors: efficient vehicles for in vitro and in vivo gene delivery. *FEBS Lett.* 504:99–103.
12. Tamm, K., A. Merits, and I. Sarand. 2008. Mutations in the nuclear localization signal of nsP2 influencing RNA synthesis, protein expression and cytotoxicity of Semliki Forest virus. *J. Gen. Virol.* 89:676–686.
13. Korobova, F., and T. Svitkina. 2010. Molecular architecture of synaptic actin cytoskeleton in hippocampal neurons reveals a mechanism of dendritic spine morphogenesis. *Mol. Biol. Cell.* 21:165–176.